Mol Breeding (2018) 38: 126
https://doi.org/10.1007/s11032-018-0882-2

Controlling population structure in the genomic prediction of tropical maize hybrids

Danilo Hottis Lyra · Ítalo Stefanine Correia Granato · Pedro Patric Pinho Morais · Filipe Couto Alves · Anna Rita Marcondes dos Santos · Xiaoqing Yu · Tingting Guo · Jianming Yu · Roberto Fritsche-Neto

Received: 8 November 2017 / Accepted: 12 September 2018 / Published online: 25 September 2018

Abstract In tropical maize breeding programs where more than two heterotic groups are crossed, factors such as population structure (PS) can influence the achievement of reliable estimates of genomic breeding values (GEBVs) for complex traits. Hence, our objectives were (i) to investigate PS in a set of tropical maize inbreds and their derived hybrids, and (ii) to control PS in genomic predictions of single-crosses considering two scenarios: applying (1) the traditional GBLUP (GB) and four adjustment methods of PS in the whole group, and (2) homogeneous- (A-GB), within- (W-GB), multi- (MG-GB), and across-group (AC-GB) analysis in stratified groups. Three subpopulations were identified in the inbred lines and hybrids based on fineSTRUCTURE results. Adding four different sets of PS as covariates to the prediction model did not improve the predictive ability (*r*). However, using non-metric multidimensional scaling and fineSTRUCTURE group clustering increased the reliability of GEBV estimation for grain yield and plant height, respectively. The W-GB analysis in the stratified groups resulted in low *r*, mostly due to the reduction of training size. On the other hand, A-GB and MG-GB showed similar *r* for both traits. However, MG-GB presented higher broad sense genomic heritabilities compared to A-GB, efficiently controlling heterogeneity of marker effects between subpopulations. The *r* of the AC-GB method was low when predicting groups genetically distant. We conclude that predicting hybrid phenotypes by using PS covariates and multi-group analysis in stratified clusters may be an efficient method, increasing reliability and predictive ability, respectively.

Keywords Stratified groups · MG-GBLUP · Across subpopulation · Linkage disequilibrium · Marker effect

Electronic supplementary material The online version of this article (https://doi.org/10.1007/s11032-018-0882-2) contains supplementary material, which is available to authorized users.

D. H. Lyra (✉) · Í. S. C. Granato · P. P. P. Morais · F. C. Alves · A. R. M. dos Santos · R. Fritsche-Neto
Luiz de Queiroz College of Agriculture, Department of Genetics, University of São Paulo, Piracicaba, São Paulo, Brazil
e-mail: danilo.hottis-lyra@rothamsted.ac.uk

D. H. Lyra
Department of Computational & Analytical Sciences, Rothamsted Research, Harpenden, UK

X. Yu · T. Guo · J. Yu
Department of Agronomy, Iowa State University, Ames, IA 50011, USA

Introduction

Tropical maize represents one of the most diverse sources of germplasm used in several plant breeding programs (Fan et al. 2015; Teixeira et al. 2015; Laborda et al. 2005). Recently, high-density single-nucleotide polymorphisms (SNPs) have been used to characterize the heterotic pools via genetic diversity (Oyekunle et al. 2015) and population structure analysis (da Silva et al. 2015; Nelson et al. 2016). Moreover, the applicability of such diversity information extends to association studies (Chen and Lipka 2016; Crossa

et al. 2007), genomic prediction (Yu et al. 2016), and germplasm architecture (Bernardo and Thompson 2016).

Population structure (PS) in maize could arise from local adaptation or diversifying selection (Orozco-Ramirez et al. 2016; Navarro et al. 2017; Bedoya et al. 2017). For the temperate maize, several subpopulations/groups (flint, dent, stiff stalk, and non-stiff stalk) were described according to morphological, genetic, and environmental adaptability characteristics (Rincent et al. 2014; Schaefer and Bernardo 2013). However, the tropical materials are not as organized as the temperate, which can be due to the stronger divergence of heterotic groups by long-term selection (Wu et al. 2016). For instance, at the International Maize and Wheat Improvement Center (CIMMYT), the development of Lowland Tropical and Subtropical/Midaltitude subgroups began in the mid-1980s (Braun et al. 1996); nonetheless, temperate materials started around 100 years ago (Unterseer et al. 2016; Wu et al. 2016). A detailed description of PS in maize lines of Brazil was reported by Laborda et al. (2005) and Lanes et al. (2014). In the last study, 81 microsatellite loci were screened concerning 90 maize parental inbreds of tropical hybrids in order to identify three heterotic pools (tropical flint, semi-flint, and semi-dent), which agreed with what has been used by Brazilian maize seed companies.

Different ways to investigate PS can be classified into either non-model-based (or non-parametric) or model-based approaches. Non-parametric methods include principal component analysis (Patterson et al. 2006; Price et al. 2006), discriminant analysis of principal components (Jombart et al. 2010), and non-metric multidimensional scaling (Zhu and Yu 2009). For model-based clustering, the algorithm in ADMIXTURE v.1.23 (Alexander et al. 2009), similar with STRUCTURE v.2.3.4, is an ordinarily used approach. Also, the recently developed ChromoPainter/fineSTRUCTURE v.2 (Lawson et al. 2012) considers linkage disequilibrium (LD) patterns in the genome, aiming to make use of haplotype structure and extracting more information from the data. Furthermore, to identify the optimal number of clusters, methods such as k-means clustering (Cros et al. 2015; Jan et al. 2016; Reif et al. 2003), ADMIXTURE cross-validation (Alexander et al. 2009), and ΔK Evanno criteria (Evanno et al. 2005) are the well-known ones in practice.

Accounting for the population structure has been proven very useful for many different applications in plant breeding, especially in association and prediction analyses. In the genomic prediction methods, one strategy is to consider PS in the design of the cross-validation scheme, for example ensuring that each subpopulation is equally represented in the training and validation sets (Albrecht et al. 2014; Guo et al. 2014). Also, several optimization criteria of the calibration set can be applied to maximize predictive ability in highly diverse panels (Isidro et al. 2015; Rincent et al. 2017, 2012). Another option is using PS as covariates in models aiming to control potential confounding factors and improve statistical power by reducing residual variance (Aschard et al. 2015). For instance, principal components (PCs) and admixture coefficients have been successfully used as fixed effects (covariates) in mixed-model equations for association studies (Price et al. 2010; Tucker et al. 2014; Yu et al. 2006) and genomic prediction (Azevedo et al. 2017; Daetwyler et al. 2012; Roorkiwal et al. 2016). On the other hand, using PCs in genomic best linear unbiased prediction (GBLUP) model may result in an ill-posed model because the PCs enter both as fixed effects and implicitly through the random effect (de los Campos and Sorensen 2014). Hence, Janss et al. (2012) proposed a reparameterized Bayesian whole-genome random regression (WGRR) model to handle this problem, drawing inferences based on all or some PCs, allowing a natural separation of across- and within-subpopulation genetic variance. In plant breeding, Guo et al. (2014) applied this model in maize and rice populations to control PS and found that within-subpopulation genetic variance contributed the majority of genomic heritability.

Furthermore, the presence of hidden or known structure and family relatedness within a breeding population is critical when evaluating genomic estimated breeding values (GEBVs), genomic heritability, and predictive ability, because it could lead to biased estimations (Isidro et al. 2015; Lehermeier et al. 2014; Spindel et al. 2015; Unterseer et al. 2014; Windhausen et al. 2012). Therefore, a standard approach to prediction analysis is partitioning the genomic variability into within- and across-group components (Technow et al. 2012). In animal breeding, within-group estimates of GEBV can be more accurate than across-group (Saatchi et al. 2011; Ventura et al. 2016), which can be due to non-persistent associations or inconsistent LD between SNPs and QTL across populations (Hayes et al. 2009; Iheshiulor et al. 2016). However, in plant breeding, exploiting within-group analyses may not

always improve predictive ability (Cros et al. 2015; Schulz-Streeck et al. 2012). It has been shown that splitting the breeding population into subgroups could lead to a reduction of population size, loss of diversity, and besides that, no correlation between marker effects is assumed in the subpopulations (Albrecht et al. 2014; Huang et al. 2016; Riedelsheimer et al. 2013). In order to overcome this last drawback, Lehermeier et al. (2015) applied a multi-group (MG-GBLUP) analysis to control heterogeneity of marker effects between subpopulations and found promising results depending on the genetic architecture of the trait. Previous reports have shown the superiority of the multi-group over within-group prediction based on predictive ability and genomic heritability (Karoui et al. 2012; Olson et al. 2012; Porto-Neto et al. 2015; Wientjes et al. 2017; Zhou et al. 2014).

In a typical maize hybrid breeding program, inbred lines from two heterotic groups are mated. However, depending on the strategy, more than two groups are used in the crossing. In this case, although two alleles may share a common genetic background in hybrids, it is essential to find patterns of PS and apply this information in genome-based predictions, as an attempt to identify high performing hybrids (Albrecht et al. 2014; Lehermeier et al. 2015). Therefore, our objectives were (i) to investigate PS in a set of tropical maize inbreds and their derived hybrids, and (ii) to control PS in genomic predictions of single-crosses considering two scenarios: applying (1) the traditional GBLUP (GB) and four adjustment methods of PS in the whole group, and (2) homogeneous- (A-GB), within- (W-GB), multi- (MG-GB), and across-group (AC-GB) analysis in stratified groups.

Materials and methods

Phenotypic data

We used 452 maize single-crosses (hybrid dataset) provided by Helix Sementes®, São Paulo, Brazil. The hybrids represent a partial diallel mating design between 128 tropical inbred lines (inbred dataset). No heterotic group information was available. The field design used was a randomized complete block with two replications. Experimental trials were carried out in five sites in southern, southeastern, and west-central regions of Brazil during the first growing season of 2014/2015. For more details about the sites, see Sousa et al. (2017). The hybrids analyzed in each location varied, thus creating an unbalanced experiment. Two-row plots of 5 m spaced 0.70 m were used. Sowing density was about 63,000 kernels per hectare, under conventional fertilization, weed, and pest control. The traits evaluated were grain yield (GY, t ha^{-1}) and plant height (PH, cm). Plots were mechanically harvested and converted to 13% moisture, and plant height measured from soil surface to the flag leaf collar on one representative plant within each plot (company criteria). We used a linear mixed model to calculate the BLUPs for hybrids, including site as a fixed effect, and hybrid and interaction as random effects. We used a factor analytic of order 1 (FA1) structure for the genotype effects across sites, and for the residual term, an unstructured (US) covariance matrix across sites. Variance components and entry-mean based heritability were obtained for GY and PH, and the significance of the random effects of hybrids was assessed by the likelihood ratio test (LRT) at 5% probability, using ASReml-R (Butler et al. 2009).

Genotypic data

The genotyping of the inbreds was performed by Affymetrix® platform, containing 614,000 SNPs (Unterseer et al. 2014). Markers with low call rate (< 95%) and with at least one heterozygous combination were removed. Imputation was done based on Wright equilibrium using snpReady-R (Granato et al. 2018). Polymorphic SNP markers were used to build the hybrid genotype dataset, deduced by combining the genotypes from its two parents. Afterwards, minor allele frequency was conducted over hybrid markers considering the threshold of 0.05, resulting in a total of 52,700 high-quality SNPs distributed in the ten maize chromosomes as follows: (1) 7015, (2) 6020, (3) 6072, (4) 5953, (5) 6431, (6) 4736, (7) 5197, (8) 4436, (9) 3529, and (10) 3311.

Linkage disequilibrium (LD) among markers may lead to unstable estimates of PS (Campoy et al. 2016; Galinsky et al. 2016). Therefore, we thinned both datasets using PLINK v.1.9 (Purcell et al. 2007) by removing SNPs that were in LD, with a pairwise r^2 value higher than 0.7 within a 50-SNP sliding window which was advanced by 10 SNPs each time. The final genomic data was 32,838 SNPs for the inbred dataset and 26,210 SNPs for the hybrid dataset, which was used as input to perform PS analysis and genomic prediction.

Inference of population structure

Inbred dataset

We used four approaches to detect PS: (a) principal component analysis (PCA), (b) non-metric multidimensional scaling (nMDS), (c) ADMIXTURE, and (d) ChromoPainter/fineSTRUCTURE. PCA was performed using SNPRelate-R (Zheng et al. 2012) in the pruned SNP data (32,838 SNPs), and the results were presented as two- and three-dimensional principal component scores plots. For nMDS analysis, labdsv-R (Roberts 2016) was used in the Rogers' distance matrix, with three dimensions, and the first two dimensions were plotted.

ADMIXTURE was used to perform a maximum likelihood estimation of individual ancestries, and ChromoPainter and fineSTRUCTURE were used to find patterns of haplotype similarity. Firstly, we applied the ChromoPainter unlinked model on haplotypes, with ten expectation maximization (EM) steps. Secondly, fineSTRUCTURE was used to perform Markov chain Monte Carlo (MCMC) analysis with 100,000 burn-in iterations and sample iterations with a thinning interval of 100. Normalization parameter c was calculated following the unlinked case, $c = 1/(N-1)$, where N is the number of individuals. Visualization of the posterior distribution of clusters was performed using the tree-building algorithm, and the number of clusters was inferred by, arbitrarily setting a cutoff in the tree.

To estimate the optimal number of clusters, we used two approaches, the cross-validation errors analyzed in ADMIXTURE, and the Bayesian information criterion (BIC) values in k-means clustering, implemented in adegenet 2.0.1-R (Jombart et al. 2015). Furthermore, to visualize the genetic differences between inbred lines, a neighbor-joining tree (NJT) was generated based on the modified Rogers' distance. We also investigated the LD structure within 70 kb of distance among all pairs of markers (32,838 SNPs), using PLINK v.1.9, and the values were reported as the average r^2 across ten chromosomes.

Hybrid dataset

We used PCA, nMDS, and fineSTRUCTURE to detect PS following the same procedure as the inbred dataset. In addition, we built an artificial ADMIXTURE coefficient for the hybrids, following the equation: $ADM_{12} = (ADM_{P1} + ADM_{P2})/2$, where ADM is the admixture coefficient of each parent, ranging from 0 to 1.

In order to visualize and describe related individuals, we used discriminant analysis of principal components (DAPCs) (Jombart et al. 2010), using the inferred groups of fineSTRUCTURE. The number of principal components to be retained in the discriminant analysis was set to 15 following alpha-score optimization, a method that finds a trade-off between discriminative power and model overfitting. We also plotted the genomic relationship matrix (GRM) by a network graph, in which two hybrids were linked when their relationship coefficient was ≥ 0.6. The networks were visualized using the igraph-R (Csardi and Nepusz 2006) with the Fruchterman Reingold layout.

Statistical models

Traditional GBLUP model

We used the additive-dominance GBLUP in the whole group (452 hybrids) ignoring the population structure by fitting the following model:

$$\hat{\boldsymbol{y}} = \boldsymbol{X\beta} + \boldsymbol{Z_a a} + \boldsymbol{Z_d d} + \varepsilon, \quad (1)$$

where $\hat{\boldsymbol{y}}$ is a vector of hybrid BLUPs, $\boldsymbol{\beta}$ is a vector of fixed effects, $\boldsymbol{a}$ is a vector of additive genetic effects on the individuals considered as random, $\boldsymbol{d}$ is the vector of dominance random effects, and ε is a vector of random residuals. $\boldsymbol{X}$, $\boldsymbol{Z_a}$, and $\boldsymbol{Z_d}$ are the incidence matrices for β, $\boldsymbol{a}$, and $\boldsymbol{d}$, respectively. The distributions were assumed as $\boldsymbol{a} \sim N(\boldsymbol{0}, \sigma_a^2 \boldsymbol{G_a})$, $\boldsymbol{d} \sim N(\boldsymbol{0}, \sigma_d^2 \boldsymbol{G_d})$, and $\varepsilon \sim N(\boldsymbol{0}, \sigma_e^2 \boldsymbol{I_n})$. $\boldsymbol{G_a}$ and $\boldsymbol{G_d}$ are the additive and dominance GRM, following the equations: $\boldsymbol{G_a} = \frac{\boldsymbol{W_A W_A'}}{tr(\boldsymbol{W_A W_A'})/m}$ and $\boldsymbol{G_d} = \frac{\boldsymbol{W_D W_D'}}{tr(\boldsymbol{W_D W_D'})/m}$, where m is the number of markers. The incidence matrices $\boldsymbol{W_A}$ and $\boldsymbol{W_D}$ were designed following VanRaden (2008) and Da et al. (2014). To build the $\boldsymbol{W_A}$ matrix, we used a genotypic incidence matrix ($\boldsymbol{S_A}$) coded as 2 for homozygote A_1A_1, 1 for heterozygote A_1A_2, and 0 for homozygote A_2A_2. For $\boldsymbol{W_D}$, the genotypic incidence matrix ($\boldsymbol{S_D}$) was coded as 0 for both homozygotes and 1 to the heterozygote.

PS covariates

We applied the Q+K model (Yu et al. 2006) on the genomic prediction of hybrids for both traits, using the

PS-related variables as fixed covariates in the GBLUP (GB) model. Hence, we used four contrasting Q approaches that includes (a) first three PCs (GB+PC), (b) three dimensions of non-metric multidimensional scaling (GB+nMDS), (c) artificial admixture coefficients (GB+ADM), and (d) a matrix of zeros and ones based on fineSTRUCTURE group clustering (GB+FINE). Furthermore, to select the top PCs (Patterson et al. 2006), we evaluated the number of statistically significant principal components, measured by the Tracy-Widom test using LEA-R (Frichot and Francois 2015) and added a varied number of PCs (3, 5, 10, 14) in GBLUP.

For the whole-group GB and GB plus PS covariates models, we evaluated the predictive ability (r). The r was measured as the Pearson's correlation of the adjusted values and predicted phenotypic values of the hybrids, obtained from 50 replications. In each replication, 75% of the single-crosses were randomly sampled to form the training set (TS) whereas the remaining hybrids constituted the validation set (VS). We used the T2 validation scenario proposed by Technow et al. (2012), in which both parents (female or male) of a single cross participate in the validation set. Also, reliability (*REL*) (Gorjanc et al. 2015) was used to compare the model performance. *REL* was calculated according to the formula: $REL = 1-\left(PEV/\sigma_g^2\right)$, where *PEV* is the variance of prediction errors of the GEBV of the hybrid ($\hat{g}_i$). Note $PEV = SD(\hat{g}_i)^2 = var(g_i - \hat{g}_i)$, where *SD* is the standard deviation. The model with the highest *REL* value presented the best precision in earlier studies (He et al. 2016; Gorjanc et al. 2015). The mean values of r and *REL* estimated from 50 replications in the independent validation were used in the overall model performance comparison. We applied Fisher's Z transformation in the predictive abilities from all models, and the means were compared by Scott-Knott's test at 5% significance. All variance components were determined using Bayesian generalized linear regression (BGLR) (Perez and de los Campos 2014) for the five mixed-models. We used a total of 30,000 MCMC iterations, 5000 for burn-in, and 5 for thinning. We also reported posterior mean estimates and standard deviations (SDs) of the broad sense genomic heritability $[H_g^2 = \left(\sigma_a^2 + \sigma_d^2\right) / \left(\sigma_a^2 + \sigma_d^2 + \sigma_e^2\right)]$, where σ_a^2, σ_d^2, and σ_e^2 are the additive, dominance, and residual variances, respectively.

Homogeneous-, within-, multi-, and across-group analysis

We used the stratified groups (subgroups) to make inferences of hybrid prediction using four main approaches, detailed in Lehermeier et al. (2015). The first is a homogeneous-group (A-GB) approach, which assumes constant marker effects across groups, which means that we use all available data (whole group), but evaluating the accuracy within subpopulations (in each group the marker effects are identical). A second method is a stratified within-group analysis (W-GB), estimating marker effects and variance components within each K separately, with a specific GRM. A third scheme is a multivariate approach (MG-GB) that uses multi-group data and accounts for heterogeneity, with population-specific marker effects that can be correlated between subpopulations. The last approach used was the across-group prediction (AC-GB), where individuals from one group were used to build the training set to predict the performances of individuals from a different group (validation set). For example, if we used K1 to predict K2 (K1→K2) subpopulation, we randomly sampled 75% of the hybrids to form the TS with K1 individuals and the rest of VS from K2.

For the homogeneous-group approach, we used the additive-dominance A-GBLUP by fitting the following model:

$$\hat{\boldsymbol{y}}_{\boldsymbol{k}} = \boldsymbol{X}_{\boldsymbol{k}}\boldsymbol{\beta}_{\boldsymbol{k}} + \boldsymbol{Z}_{\boldsymbol{a}_{\boldsymbol{k}}}\boldsymbol{a}_{\boldsymbol{k}} + \boldsymbol{Z}_{\boldsymbol{d}_{\boldsymbol{k}}}\boldsymbol{d}_{\boldsymbol{k}} + \boldsymbol{\varepsilon}_{\boldsymbol{k}}, \quad (2)$$

where $\hat{\boldsymbol{y}}_{\boldsymbol{k}}$ is the n_k-dimensional vector of hybrid BLUPs of subpopulation k, $\boldsymbol{\beta}_{\boldsymbol{k}}$ is the p_k-dimensional vector of fixed effects common for all k subpopulations, $\boldsymbol{a}_{\boldsymbol{k}}$ is the n_k-dimensional vector of additive genetic of random effects on the individuals for subpopulation k, $\boldsymbol{d}_{\boldsymbol{k}}$ is the n_k-dimensional vector of dominance random effects for subpopulation k, and $\boldsymbol{\varepsilon}_{\boldsymbol{k}}$ is n_k-dimensional vector of random residuals belonging to subpopulation k. $\boldsymbol{X}_{\boldsymbol{k}}$, $\boldsymbol{Z}_{\boldsymbol{a}}$, and $\boldsymbol{Z}_{\boldsymbol{d}}$ are the incidence matrices for $\boldsymbol{\beta}_{\boldsymbol{k}}$, $\boldsymbol{a}_{\boldsymbol{k}}$, and $\boldsymbol{d}_{\boldsymbol{k}}$, respectively. The complete vector $\boldsymbol{a} = \left(\boldsymbol{a}_{\boldsymbol{1}}^{'}, \ldots, \boldsymbol{a}_{\boldsymbol{K}}^{'}\right)$ is assumed to follow $\boldsymbol{a}|\sigma_a^2 \sim MVN_{n\times n}\left(\boldsymbol{0}, \sigma_a^2\boldsymbol{G}_{\boldsymbol{a}}\right)$, and the vector $\boldsymbol{d} = \left(\boldsymbol{d}_{\boldsymbol{1}}^{'}, \ldots, \boldsymbol{d}_{\boldsymbol{K}}^{'}\right)$ is assumed to follow $\boldsymbol{d}|\sigma_d^2 \sim MVN_{n\times n}\left(\boldsymbol{0}, \sigma_d^2\boldsymbol{G}_{\boldsymbol{d}}\right)$. $\boldsymbol{G}_{\boldsymbol{a}}$ and $\boldsymbol{G}_{\boldsymbol{d}}$were built following the same parameterization as those defined in model (1). It is worth noting that the residuals are assumed to follow a normal distribution with mean 0 and subpopulation-specific variance as

$\boldsymbol{\varepsilon_k} \sim MVN_{n_k \times n_k}\left(\mathbf{0}, \sigma^2_{\varepsilon_k}\boldsymbol{I}\right)$. We assigned a scaled inverse chi-square prior distribution with degrees of freedom (df_1) and scale parameter (S_1) of $\sigma^2_a \sim \chi^{-2}(df_1, S_1)$, $\sigma^2_d \sim \chi^{-2}(df_1, S_1)$, and $\sigma^2_{\varepsilon_k} \sim \chi^{-2}(df_0, S_0)$ for σ^2_a, σ^2_d, and $\sigma^2_{\varepsilon_k}$, respectively.

For the within-group method, we used the additive-dominance W-GBLUP by fitting the following model:

$$\hat{\boldsymbol{y}}_{\boldsymbol{k}} = \boldsymbol{X_k}\boldsymbol{\beta_k} + \boldsymbol{Z}_{\boldsymbol{a_k}}\boldsymbol{a_k} + \boldsymbol{Z}_{\boldsymbol{d_k}}\boldsymbol{d_k} + \boldsymbol{\varepsilon_k}, \quad (3)$$

where $\hat{\boldsymbol{y}}_{\boldsymbol{k}}$, $\boldsymbol{a_k}$, $\boldsymbol{d_k}$, and $\boldsymbol{\varepsilon_k}$ are the same as those defined in model (2). However, $\boldsymbol{\beta_k}$ is the p_k-dimensional vector of fixed effects specific for subpopulation k, and the vectors of additive and dominance effects for each subpopulation are assumed to follow different independent normal distributions: $\boldsymbol{a_k}|\sigma^2_{a_k} \sim MVN_{n_k \times n_k}\left(\mathbf{0}, \sigma^2_{a_k}\boldsymbol{G_{a_k}}\right)$ and $\boldsymbol{d_k}|\sigma^2_{d_k} \sim MVN_{n_k \times n_k}\left(\mathbf{0}, \sigma^2_{d_k}\boldsymbol{G_{d_k}}\right)$, where $\boldsymbol{G_{a_k}}$ and $\boldsymbol{G_{d_k}}$ is the genomic relationship matrix among individuals of the kth subpopulation, and $\sigma^2_{a_k}$ and $\sigma^2_{d_k}$ are the additive and dominance variances of the kth subpopulation. Residuals are assumed to follow a normal distribution with mean 0 and subpopulation-specific variance as $\boldsymbol{\varepsilon_k} \sim MVN_{n_k \times n_k}\left(\mathbf{0}, \sigma^2_{\varepsilon_k}\boldsymbol{I}\right)$. As in A-GB, we assigned a scaled inverse chi-square prior distribution with degrees of freedom (df_1) and scale parameter (S_1) of $\sigma^2_a \sim \chi^{-2}(df_1, S_1)$, $\sigma^2_d \sim \chi^{-2}(df_1, S_1)$, and $\sigma^2_{\varepsilon_k} \sim \chi^{-2}(df_0, S_0)$ for σ^2_a, σ^2_d, and $\sigma^2_{\varepsilon_k}$, respectively. Also, to each group k, marker effect based on the adjusted entry means for grain yield, and plant height was estimated, using rrBLUP-R (Endelman 2015). Besides that, LD structure was investigated within 70 kb of distance between all pairs of markers, and the values were reported as the average r^2 across ten chromosomes.

For the additive-dominance MG-GBLUP approach, we used the following model:

$$\hat{\boldsymbol{y}}_{\boldsymbol{k}} = \boldsymbol{X_k}\boldsymbol{\beta_k} + \boldsymbol{Z}_{\boldsymbol{a_k}}\boldsymbol{a_k} + \boldsymbol{Z}_{\boldsymbol{d_k}}\boldsymbol{d_k} + \boldsymbol{\varepsilon_k}, \quad (4)$$

where $\hat{\boldsymbol{y}}_{\boldsymbol{k}}$, $\boldsymbol{\beta_k}$, $\boldsymbol{a_k}$, $\boldsymbol{d_k}$, and $\boldsymbol{\varepsilon_k}$ are the same as those defined in model (3). However, the model estimates population-specific marker effects allowing for correlations of effects between groups. In this case, the complete vector of the genomic values of individuals in each group is an augmented form ($n.\ K$), $\boldsymbol{a}^* = \left(\boldsymbol{a}_1^{*\prime}, \ldots, \boldsymbol{a}_K^{*\prime}\right)$ and $\boldsymbol{d}^* = \left(\boldsymbol{d}_1^{*\prime}, \ldots, \boldsymbol{d}_K^{*\prime}\right)$, with the additive and dominance effects following a multivariate normal distribution $\boldsymbol{a^*} \mid \sum_a \sim MVN_{n.\ k \times n.\ k}(\mathbf{0}, \sum_a \otimes \boldsymbol{G_a})$, and $\boldsymbol{d^*} \mid \sum_d \sim MVN_{n.\ k \times n.\ k}(\mathbf{0}, \sum_d \otimes \boldsymbol{G_d})$. $\sum_a$ and $\sum_d$ are an unstructured (US) genomic variance-covariance matrix (V-COV) among subpopulations. Differently, from A-GB and W-GB, we assumed a correlation between residuals and following a normal distribution with subpopulation-specific residual variances, $\boldsymbol{\varepsilon_k} \sim MVN_{n_k \times n_k}(\mathbf{0}, \sum_e \otimes \boldsymbol{D_e})$, where $\sum_e$ is an US V-COV of residuals. The hyperparameters of the prior distributions of the variance components were chosen according to the inverse Wishart, $\sum_a \sim W^{-1}(\Psi, \nu)$, where the scale matrix Ψ was a diagonal with entries equal to $\Psi = 0.5 \times (\nu + k + 1)$, and the degrees of freedom (ν) were set to $\nu = k + 3$, where k is the number of groups (Lehermeier et al. 2015). The same approach was assumed to the dominance and residual variances.

The predictive ability of A-GB, W-GB, and MG-GB were assessed with 50 replications from independent T2 validation scenario, randomly sampling 75% of the hybrids to form the TS and the rest of VS. We applied Fisher's Z transformation in the predictive abilities from all models, and the means were compared by Scott-Knott's test at 5% significance. A total of 30,000 MCMC iterations, 5000 for burn-in, and 5 for thinning were used to estimate the parameters using the MTM-R package. We reported posterior mean estimates and standard deviations of the H^2_g for each k.

Results

Inbred PS

In the ADMIXTURE analysis, the optimal number of clusters was L = 7 with the smallest cross-validation error (Supplemental Fig. S1a, Fig. S2). The k-means clustering identified L = 3 with the smallest BIC value (Supplemental Fig. S1b). The fineSTRUCTURE result is a coancestry heatmap, which shows the amount of shared genetic chunks between the inbred lines (Fig. 1a). We defined a cutoff on the maximum a posteriori tree with three groups (L), each containing 100 (L1), 13 (L2), and 15 (L3) inbred lines. In within-group L1, five distinct subgroups were revealed, explaining the seven groups identified in the ADMIXTURE results (Supplemental Fig. S2a). Moreover, PCA, nMDS, and cluster (NJT) analysis also revealed levels of PS identified in both model-based clusterings (Fig. 1; Supplemental Fig. S3a). The first two PCs explained

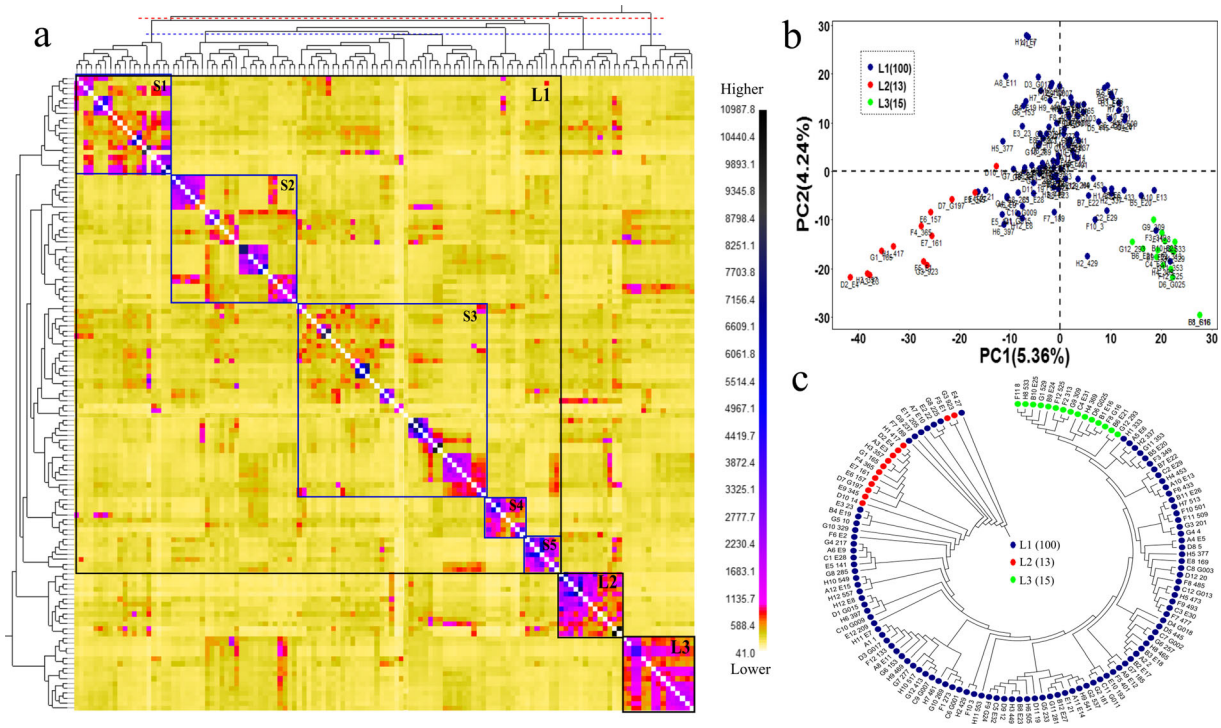

Fig. 1 Population structure analysis in 128 tropical maize inbred lines. **a** Coancestry heatmap of fineSTRUCTURE unlinked model. The scale shows lower (white) to higher (black) amount of shared genetic chunks between the inbred lines. On the left and top is the maximum a posteriori (MAP) tree. The dashed red line is the cutoff threshold splitting L1, L2, and L3 groups. Dashed blue line clustered the subgroups S1, S2, S3, S4, and S5. **b** First two principal components. **c** Circular neighbor-joining tree based on modified Rogers' distance

5.36% and 4.24% of the total variance, clearly splitting the groups along the axis. However, nMDS analysis revealed that L1 and L3 were clustered together, but separated from L2. The relationship between LD and physical distance was plotted (Supplemental Fig. S3b), and the LD decayed faster with the r^2 dropping to half its maximum value within 1.3 kb.

Hybrid PS

The unlinked coancestry heatmap of fineSTRUCTURE clustered hybrids into three groups (K), containing 113 (K1), 121 (K2), and 218 (K3) hybrids (Fig. 2a). Three subgroups of within-group K1 were also clearly shown. In the artificial admixture coefficients (Fig. 2b), we found a mixture of groups in the hybrids. PCA and nMDS dots were color-coded based on the fineSTRUCTURE group clustering. The first two PCs explained 7.40% and 6.05% of the total variance (Fig. 2c). Furthermore, the 3-D PCA score plot (Supplemental Fig. S4a) revealed a clear separation of K1 from K2, wherein PC1, PC2, and PC3 together explained 18.3% of the data variation. The within-group individuals of K1 were spread along the axis (blue density plot), confirming the subgroups identified in fineSTRUCTURE (Fig. 2a; S4a). In addition, a pattern also was detected for nMDS analysis (Fig. 2d). Network graph revealed that individuals from K2 and K3 are more related according to the GRM (Fig. 2e). The DAPC plot (Supplemental Fig. S4b) using two discriminant functions indicated that K1 were highly discriminated from K2, with reliable separation along the principal component axes. The plot did not reveal high discrimination between K2 and K3, since overlapping existed between groups.

Hybrid prediction along PS covariates

From the phenotypic analysis, it was found significant differences in the hybrids by the likelihood ratio test ($P < 0.05$), for GY and PH. Entry-mean based heritability was 0.77 for GY and 0.86, reflecting the good accuracy of the phenotypic evaluation. The adjusted values for GY varied from 3.39 to 9.37 t ha^{-1}, and for PH from 185 to 277 cm.

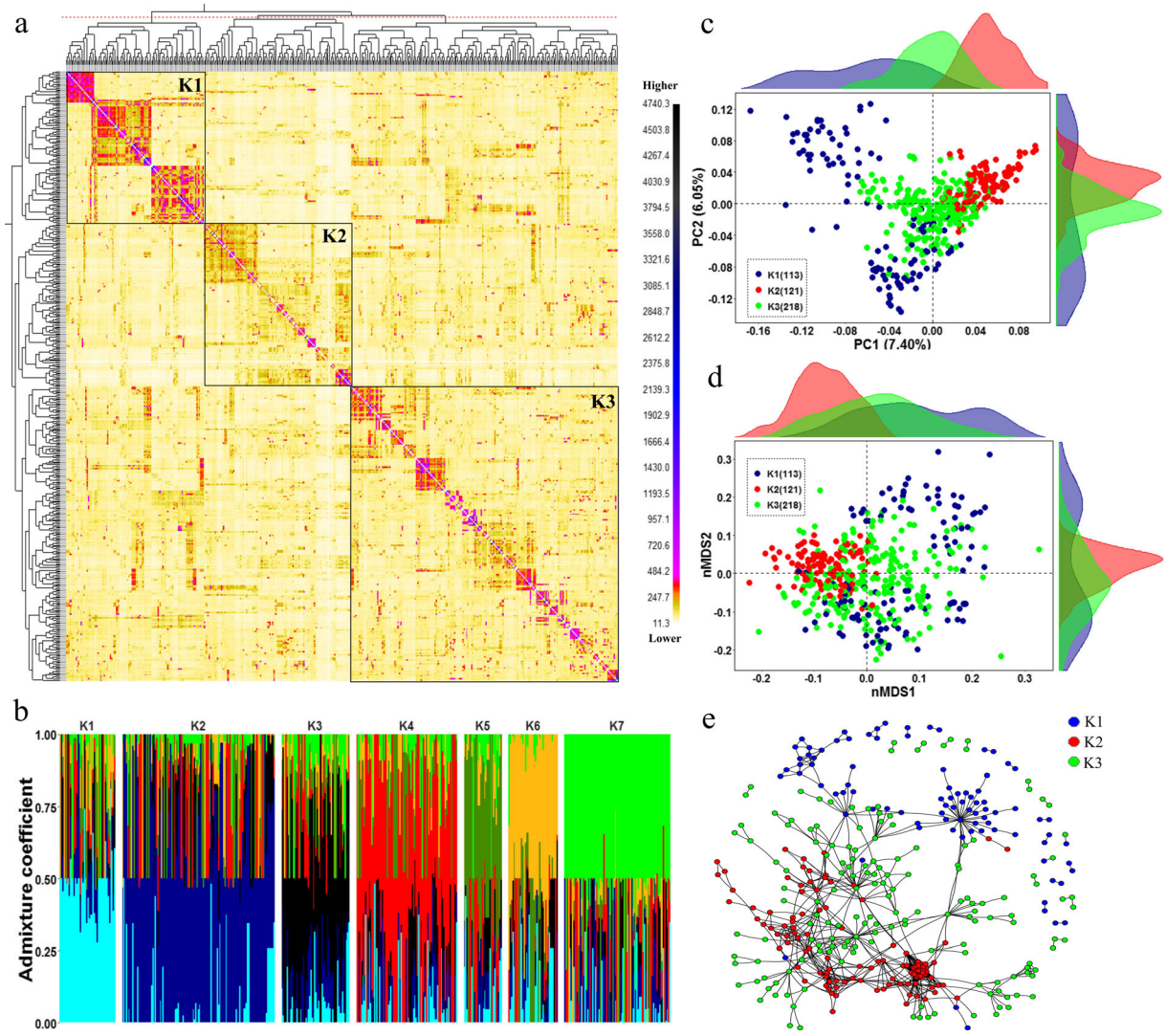

Fig. 2 Population structure analysis in 452 tropical maize single-cross hybrids. **a** Coancestry heatmap of fineSTRUCTURE unlinked model. The scale shows lower (white) to higher (black) amount of shared genetic chunks between the individuals. On the left and top is the maximum a posteriori (MAP) tree. The dashed red line is the cutoff threshold splitting K1, K2, and K3 groups. **b** Artificial admixture coefficients, where each color represents a group (K1-K7). **c** First two principal components, applied to raw SNP data (32,838 SNPs). The percentages in parentheses in the axis titles represent the variance explained by each of the two principal components. **d** First two non-metric multidimensional scaling (nMDS) dimensions, applied to Rogers' distance matrix. **e** Network representation of the GRM, where individuals were linked when their relationship coefficient was ≥ 0.6 (not all hybrids are shown). Colors in **b**, **c**, and **e** indicate three groups clustered from fineSTRUCTURE results. The number of hybrids per group is indicated in parenthesis. Density plot shows the distribution of individuals in each group

From the prediction analysis, we did not observe significant differences from Scott-Knott's test ($P < 0.05$) between the values of predictive ability (r) among all tested models for both traits (Figs. 3a; 4a). For instance, the r reached similar values of 0.74 for GY and 0.80 for PH for all models. In this case, there was no advantage of adding PS covariates in the prediction approach. However, it is important to highlight that the highest *REL* were observed using nMDS and FINE as covariates to predict GY (Supplemental Fig. S5a). For PH, FINE and ADM were the best models regarding *REL* (Supplemental Fig. S5b). Besides, estimates of broad sense genomic heritability varied slightly among models for both traits (Supplemental Fig. S6; Supplemental Fig. S7). Based on the Tracy-Widom test, the significant axes of variation to account for the

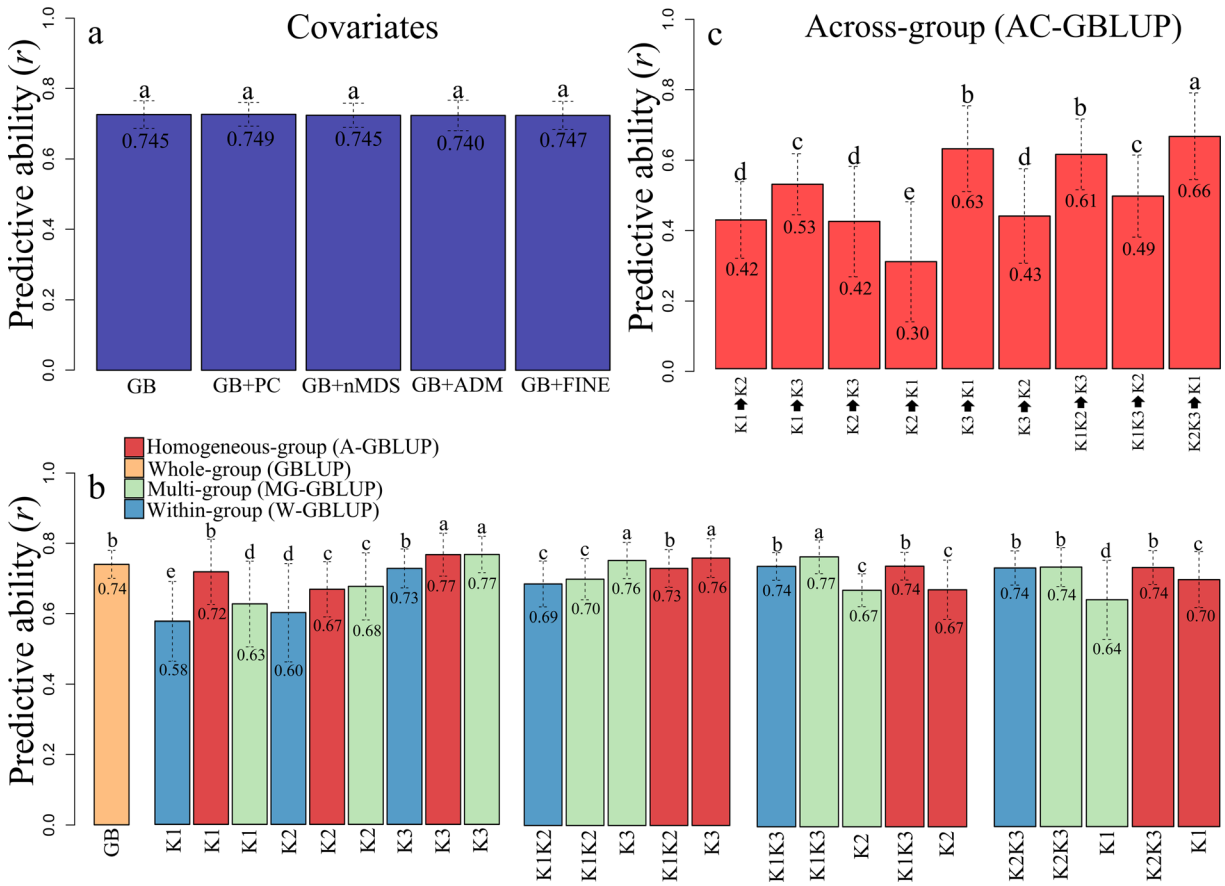

Fig. 3 Comparison of predictive ability (*r*) for grain yield. **a** GBLUP (GB) model and GB with four fixed covariates: principal components (GB+PC), non-metric multidimensional scaling dimensions (GB+nMDS), admixture coefficients (GB+ADM), and fineSTRUCTURE group clustering (GB+FINE). **b** GB, homogeneous- (A-GBLUP), within- (W-GBLUP), and multi-group (MG-GBLUP) analysis for K1, K2, K3, K1K2, K1K3, and K2K3 groups. **c** Across-group (AC-GBLUP) analysis for nine prediction schemes. Data are mean ± standard deviation (SD) estimated from 50 replications in independent validation. Letters above bars indicate significant differences between models' predictive abilities from Scott-Knott test ($P < 0.05$)

genetic structure were 14 (Supplemental Fig. S8a). For both traits, the predictive ability values slightly decreased when added more than three PCs in GBLUP model (Supplemental Fig. S8b), showing that three PCs in the model could be efficient to account population structure.

Subgroup prediction

We used within-group (K1, K2, K3, K1K2, K1K3, and K2K3 subpopulations) hybrids to investigate the predictive ability and broad sense genomic heritability for GY and PH. The highest *r* was observed when combining K2 plus K3 for GY ($r = 0.74$) and PH ($r = 0.80$), reaching similar values to the whole-group prediction (Figs. 3b; 4b). As expected, A-GB and MG-GB presented significantly higher values of *r* relative to W-GB for most of the groups. However, A-GB and MG-GB yielded similar values of *r* for all traits and groups, but in some cases, the MG-GB significantly outperformed the A-GB, and vice versa. For instance, the *r* reached values of 0.78, 0.80, and 0.84 in the K3 group using the within-, homogeneous-, and multi-group analysis for PH. We also observed that combining the subgroups K1K2+K3 and using the MG-GB model significantly improved the *r* for K3 ($r = 0.84$) compared to the whole-group prediction ($r = 0.79$), remaining similar values for the K1K2 group ($r = 0.76$) for plant height (Fig. 4b). For both traits, lower estimates of H_g^2 were observed from W-GB compared to A-GB and MG-GB (Supplemental Fig. S6b; Supplemental Fig. S7b). For

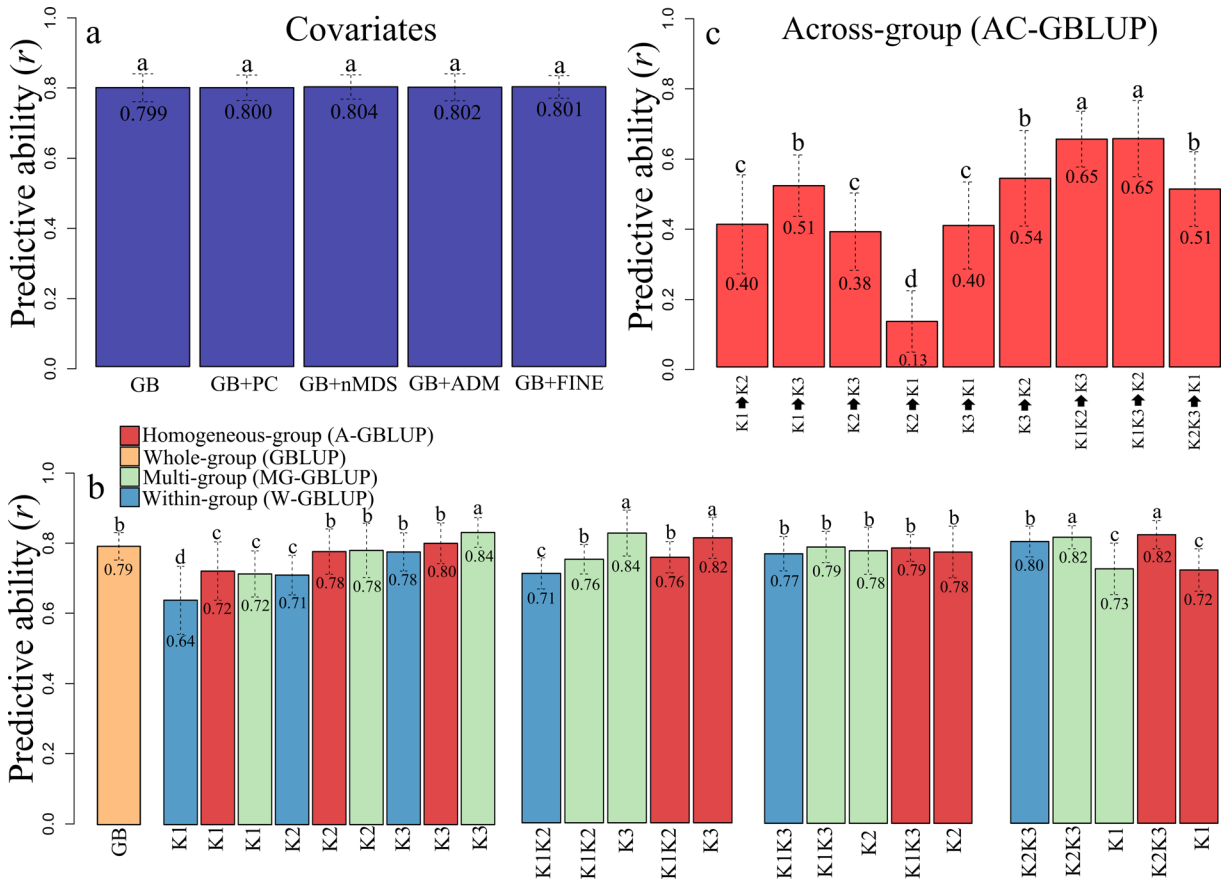

Fig. 4 Comparison of predictive ability (r) for plant height. **a** GBLUP (GB) model and GB with four fixed covariates: principal components (GB+PC), non-metric multidimensional scaling dimensions (GB+nMDS), admixture coefficients (GB+ADM), and fineSTRUCTURE group clustering (GB+FINE). **b** GB, homogeneous- (A-GBLUP), within- (W-GBLUP), and multi-group (MG-GBLUP) analysis for K1, K2, K3, K1K2, K1K3, and K2K3 groups. **c** Across-group (AC-GBLUP) analysis for nine prediction schemes. Data are mean ± standard deviation (SD) estimated from 50 replications in independent validation. Letters above bars indicate significant differences between models' predictive abilities from Scott-Knott test ($P < 0.05$)

example, the H_g^2 for PH using the whole-group (GB) was 0.86, and for W-GB was 0.71 while MG-GB was 0.89 for the K1 group. Moreover, MG-GB presented higher H_g^2 with lower SD compared to A-GB showing better model fit to the training data.

We also used eight across-group (K1 → K2, K1 → K3, K2 → K3, K2 → K1, K3 → K1, K3 → K2, K1K2 → K3, K1K3 → K2, and K2K3 → K1) prediction schemes (Figs. 3c; 4c). As expected, we observed lower r from AC-GB compared to the whole-group (traditional GBLUP), W-GB, and MG-GB for both traits. It is important to note that the r was low when predicting groups genetically distant (Fig. 2). For example, using K1 → K2 and the opposite (K2 → K1), the r for GY was 0.42 and 0.30, respectively. The significant highest r was observed when predicting K2K3 → K1 ($r = 0.66$) for GY, and K1K2 → K3 ($r = 0.65$) and K1K3 → K2 ($r = 0.65$) for PH.

The relationship between LD and physical distance (kb) was plotted for K (452), K1 (113), K2 (121), and K3 (218) (Fig. 5a). LD (r^2) rapidly decayed following the highest number of individuals inside the group. Yan et al. (2009) showed the same tendency working with a diverse global maize collection. For K, K1, K2, and K3 the LD decayed with the r^2 dropping to half their maximum value within 5.5, 6.5, 10, and 11.5 kb, respectively. Additive marker effects distribution estimated across the groups were different for GY, but it was similar for PH, in all ten chromosomes (Fig. 5b, c). Pearson correlation between group SNP effect for GY was 0.27 (K1-K2), 0.46 (K1-K3), and 0.14 (K2-K3). For PH, the r was

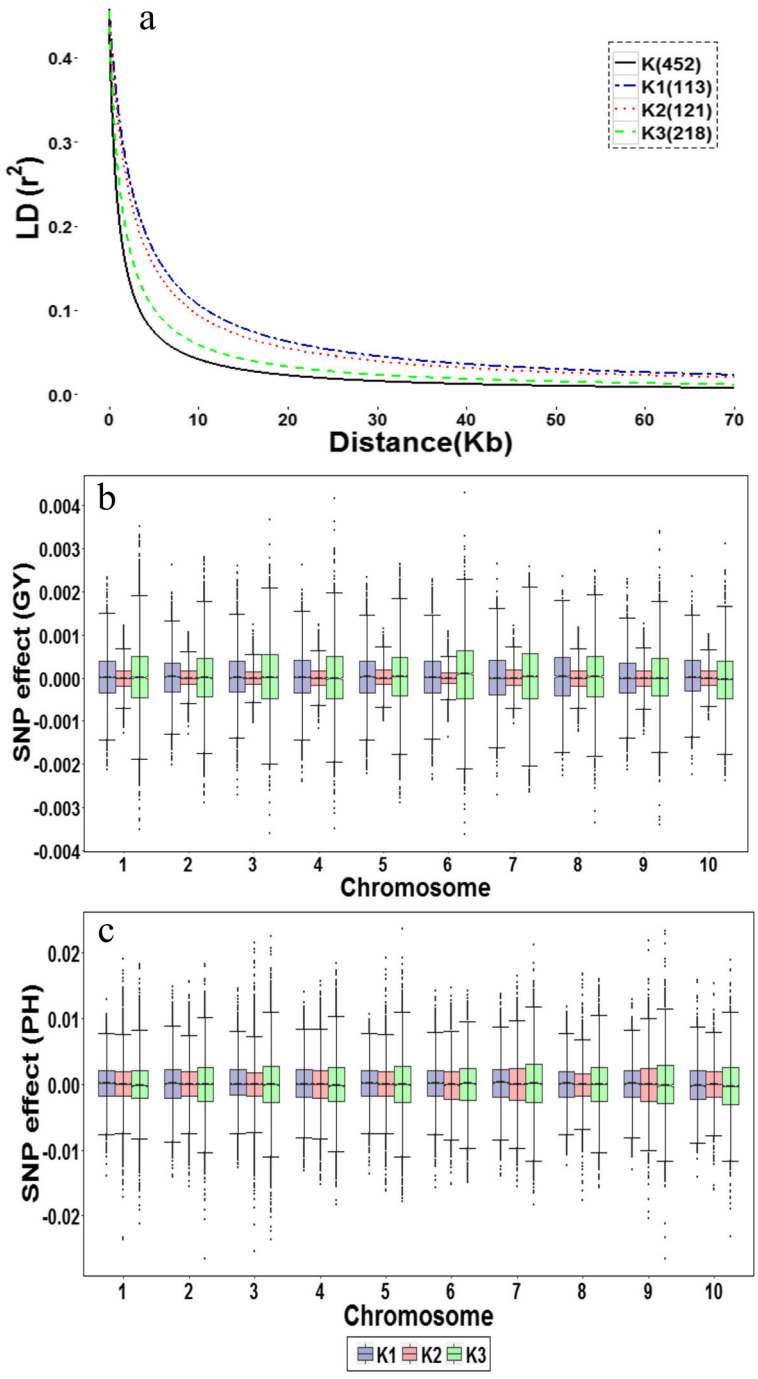

Fig. 5 **a** Pattern of linkage disequilibrium (LD) within 70 kb of distance among all pairs of markers (26 K SNPs) for 452(K), 113(K1), 121(K2), and 218(K3) individuals. Values reported are the average r^2 across ten chromosomes. Boxplots of additive marker effect estimates for **b** GY and **c** PH, for K1, K2, and K3 groups

0.33 (K1-K2), 0.38 (K1-K3), and 0.46 (K2-K3). Posterior mean estimates and posterior SD of the genomic correlations from MG-GB for GY varied among the three groups 0.34 ± 0.14 (K1-K2), 0.75 ± 0.09 (K1-K3), and 0.48 ± 0.15 (K2-K3). For PH, the values were 0.31 ± 0.16 (K1-K2), 0.74 ± 0.10 (K1-K3), and 0.51 ± 0.14 (K2-K3). Thus, the estimated genomic correlations between subpopulations K1-K3 was high for both traits, which is agreement with the GRM (Fig. 2e).

Discussion

The most common source of tropical germplasm found in the breeding programs are Tusón, Tuxpeño, Antigua Composite, Suwan-1, and Cuban Flint (also called Cateto in Brazil) (Hallauer and Carena 2014; Laborda et al. 2005), and as observed in previous studies, the number of subgroups inside tropical and subtropical still diverge (Molin et al. 2013; Reif et al. 2003; Wu et al. 2016; Ertiro et al. 2017). In the present study, 128 tropical inbred lines were characterized using k-means clustering and two model-based approaches to identify groups/clusters. Based on k-means, we classified three groups, which were consistent according to fineSTRUCTURE (Fig. 1a) and PCA (Fig. 1b). Another way to visualize the structure of populations is by the extent of linkage disequilibrium, which influences the resolution of the genome-wide analysis (Yang et al. 2011). In our study, the LD decayed within 1.3 kb (Supplemental Fig. S3b), which was consistent with the findings of Unterseer et al. (2014). These authors worked with 285 temperate and tropical maize lines genotyped with 600 K SNPs, and found L = 7 in ADMIXTURE, and observed fastest LD decay in (sub)tropical lines (70 kb) explained by the high heterogeneity inside the groups. Chia et al. (2012) and Yan et al. (2009) also found fastest LD decay within distances between 5 and 10 kb, respectively, in highly diverse tropical maize lines.

Recently, in an applied breeding scheme, Edriss et al. (2017) studied genomic prediction of tropical maize hybrids generated from 2022 diverse breeding lines from five subpopulations, demonstrating the importance of PS in genomic studies. Thus, it is common verifying PS among inbred lines to explore heterosis in divergent parental crossing (Fernandes et al. 2015; Mundim et al. 2015). However, in tropical maize breeding, hybrids could be generated from various heterotic parent groups, reflecting in high levels of structuring, confirming our results identified from fineSTRUCTURE, PC, and DAPC results (Fig. 2 and Supplemental Fig. S4). For example, within-group K1 (Fig. 2a) revealed three distinct subgrouping, which can be identified in 2-D (Fig. 2c) and 3-D (Supplemental Fig. S4) PCA graph. Also, estimates of genomic correlations based on the variance-covariance matrix between subpopulations show the extent of genetic heterogeneity between groups, corresponding to the marker effects correlations (Lehermeier et al. 2015). In our work, the estimated genomic correlations between subpopulations K1-K3 was high while the group K1-K2 was low for both traits. According to Lehermeier et al. (2015), those correlations between groups are trait-specific, being affected by the similar or contrasting values of QTL effects, epistasis, dominance, and by differences in marker-QTL LD between subgroups.

In our work, both traits showed high values of predictive ability and genomic heritability for GY (0.74; 0.79) and PH (0.80; 0.86) from traditional GBLUP (Figs. 3, 4; Supplemental Fig. S7, Supplemental Fig. S8). Similar findings were observed by Maenhout et al. (2010), Massman et al. (2013), and Santos et al. (2016). Moreover, the methods GBLUP, PC, nMDS, ADM, and FINE were compared regarding *r* and *REL*. There was no advantage of adding PS covariates in the prediction model based on *r*. Thus, one explanation could be the fact that the GRM implicitly captured the genetic variation from PS and admixture of the hybrids. Another reason could be the similarity in the mean performance of the traits between the subpopulation. According to Isidro et al. (2015) and Windhausen et al. (2012) traits are primarily impacted by PS. Therefore, predictive abilities depend on the interaction of trait architecture and levels of PS. On the other hand, including PS covariates reported herein showed better performance concerning reliability, which could substantially reduce the standard error of the genetic variant association and, consequently, increase the accuracy of GEBV estimation. As a consequence, possible changes of individual ranking could be observed in the models with and without PS correction, which is in agreement with Azevedo et al. (2017).

Several studies have been successfully conducted including PC as covariates in GWAS analysis (Sukumaran et al. 2015; Wang et al. 2011; Zhang et al. 2016). However, in genomic prediction studies, adding PC eigenvectors in the model have shown low *r* or at least the same value (Daetwyler et al. 2012; Newell and Jannink 2014). As already reported by Janss et al. (2012) and de los Campos and Sorensen (2014), the PCs added as fixed effects in the GBLUP enter twice in the model, causing misleading interpretations. On the other hand, Roorkiwal et al. (2016) studied a collection of 320 elite breeding chickpea lines including admixture coefficients (PS covariable) as fixed effect in the RR-BLUP, and found that the predictive abilities improved slightly for days to maturity (DM), days to flowering (DF), and seed dry weight (SDW). In addition, Azevedo

et al. (2017) simulated four scenarios including PCs and eigenvectors into GBLUP model and found higher estimates of *r* compared to the model with no PS correction. In our work, even finding structuring in PC plot (Fig. 2c), including the first three PCs did not change predictive ability scenario for both traits (Figs. 3a; 4a). Furthermore, we used Tracy-Widom test to select the top principal components, but the *r* slightly decreased when added the first 5, 10, and 14 significant PCs in GBLUP model for both traits (Supplementary Fig. S8b). These results are in agreement with Azevedo et al. (2017), and Daetwyler et al. (2012) who observed a decline of *r* as an increasing number of PC was fitted into the model. Therefore, the main advantage of PS correction for long-term genomic prediction is that the estimated marker effects could potentially be valid for some generations ahead (training set), saving time, and resources in the re-estimation of new effects of markers (Crossa et al. 2007, 2010; Guo et al. 2014; Isidro et al. 2015; Lehermeier et al. 2015; Windhausen et al. 2012; Azevedo et al. 2017).

The prediction including three nMDS dimensions performed better than the others methods of GY regarding reliability. In a GWAS analysis, Zhu and Yu (2009) compared nMDS and PC and found an increase in power and a decrease in false positive rate using nMDS associated with genomic kinship. Further, Sukumaran et al. (2012) worked with PS of 300 wheat lines for ten grain quality traits and tested three mixed models including admixture coefficients, nMDS, and PCA as fixed covariates in GWAS analysis. The authors found nMDS as the best approach for the amount of phosphorus (P). On the other hand, in our results, ADM was the lowest ranked method so far according to *REL* for GY. In contrast, for PH showed better performance compared to GBLUP. In animal prediction, Thomasen et al. (2013) studied US and Danish Jersey cattle by including admixture coefficients estimated from STRUCTURE in genomic prediction models and did not find any improvement of prediction reliabilities.

From our findings, predictive ability was significantly higher in A-GB and MG-GB when compared with W-GB for both traits (Figs. 3b; 4b). According to Lehermeier et al. (2015), MG-GB allows subpopulation-specific marker effects, borrowing the information between subpopulations. In contrast, within-group prediction (W-GB) reduces training size, nevertheless, increases the relationship between genotypes (Iheshiulor et al. 2016; Lehermeier et al. 2015; Mendes and de Souza 2016; Riedelsheimer et al. 2012; Huang et al. 2016). Schulz-Streeck et al. (2012) found better predictive ability joining all populations derived from five biparental populations of maize. Riedelsheimer et al. (2012) also studied PS splitting the whole population in within-group of related lines and showed that population structuring reduced predictive ability in 3.6% for SNPs relative to the whole population. In our study, higher estimates of *r* were observed from MG-GB in K3 group, for GY (0.77) and PH (0.84) relative to the whole group from traditional GBLUP and GB plus PS covariables, showing the efficiency of the method. We also observed that combining subgroups (K1K2+K3) significantly improved the *r* for K3 in both traits (Figs. 3b; 4b). Another way to visualize the impact of PS in the subgroups prediction is to measure the extent of genomic heritability. In our results, the H_g^2 for PH using the whole group (GB) was 0.86, for W-GB was 0.71, and A-GB was 0.77 while MG-GB was 0.89 for the K1 group (Supplemental Fig. S6b; Supplemental Fig. S7b). This agrees with the results reported by Guo et al. (2014) and Lehermeier et al. (2015), in which the PS showed a significant impact on genomic heritability.

In our study, as expected, we observed a considerable decrease in predictive ability and genomic heritability by the across-group (AC-GB) prediction for both traits compared to the others approaches (Figs. 3b; 4b; Supplemental S6b; Supplemental S7b). This could be related to the non-consistent additive marker effects between the subgroups for both traits, especially for GY (Fig. 5b, c). Also, this result could be justified by the low relatedness of the individuals between training and validation and different marker effects between groups (Habier et al. 2007). Similar findings were observed by Guo et al. (2014) who reported more substantial reductions in predictive ability due to the correction for PS in across-subpopulations, and Mendes and de Souza (2016) who studied PS within and across groups from 250 tropical maize single-crosses genotyped with 614 AFLP marker, finding high accuracy estimates for within-group prediction.

Conclusion

Our results suggest that there was no advantage of adding population structure covariates in the prediction

model based on predictive ability. However, using non-metric multidimensional scaling and fineSTRUCTURE group clustering increased the reliability of GEBV estimation for grain yield and plant height. Furthermore, applying the multi-group method in stratified groups may be an efficient method, significantly increasing the predictive ability and genomic heritability compared to the whole-, within-, and across-group prediction.

Funding This project was supported by the São Paulo Research Foundation-FAPESP (Process: 2013/24135-2; 2014/26326-2; 2015/14376-8) and Coordination for the Improvement of Higher Level Personnel (CAPES).

References

Albrecht T, Auinger HJ, Wimmer V, Ogutu JO, Knaak C, Ouzunova M, Piepho HP, Schon CC (2014) Genome-based prediction of maize hybrid performance across genetic groups, testers, locations, and years. Theor Appl Genet 127(6):1375–1386

Alexander DH, Novembre J, Lange K (2009) Fast model-based estimation of ancestry in unrelated individuals. Genome Res 19(9):1655–1664

Aschard H, Vilhjalmsson BJ, Joshi AD, Price AL, Kraft P (2015) Adjusting for heritable covariates can bias effect estimates in genome-wide association studies. Am J Hum Genet 96(2): 329–339

Azevedo CF, de Resende MDV, Silva FFE, Nascimento M, Viana JMS, Valente MSF (2017) Population structure correction for genomic selection through eigenvector covariates. Crop Breed Appl Biot 17(4):350–358

Bedoya CA, Dreisigacker S, Hearne S, Franco J, Mir C, Prasanna BM, Taba S, Charcosset A, Warburton ML (2017) Genetic diversity and population structure of native maize populations in Latin America and the Caribbean. PLoS One 12(4): e0173488

Bernardo R, Thompson AM (2016) Germplasm architecture revealed through chromosomal effects for quantitative traits in maize. Plant Genome 9(2):1–11

Braun HJ, Rajaram S, vanGinkel M (1996) CIMMYT's approach to breeding for wide adaptation. Euphytica 92(1–2):175–183

Butler DG, Cullis BR, Gilmour AR, Gogel BJ (2009) ASReml-R reference manual. Department of Primary Industries, Queensland

Campoy JA, Lerigoleur-Balsemin E, Christmann H, Beauvieux R, Girollet N, Quero-Garcia J, Dirlewanger E, Barreneche T (2016) Genetic diversity, linkage disequilibrium, population structure and construction of a core collection of *Prunus avium* L. landraces and bred cultivars. BMC Plant Biol 16:49

Chen AH, Lipka AE (2016) The use of targeted marker subsets to account for population structure and relatedness in genome-wide association studies of maize (*Zea mays* L.). G3-Genes Genom Genet 6(8):2365–2374

Chia JM, Song C, Bradbury PJ, Costich D, de Leon N, Doebley J, Elshire RJ, Gaut B, Geller L, Glaubitz JC, Gore M, Guill KE, Holland J, Hufford MB, Lai JS, Li M, Liu X, Lu YL, McCombie R, Nelson R, Poland J, Prasanna BM, Pyhajarvi T, Rong TZ, Sekhon RS, Sun Q, Tenaillon MI, Tian F, Wang J, Xu X, Zhang ZW, Kaeppler SM, Ross-Ibarra J, McMullen MD, Buckler ES, Zhang GY, Xu YB, Ware D (2012) Maize HapMap2 identifies extant variation from a genome in flux. Nat Genet 44(7):803–U238

Cros D, Denis M, Sanchez L, Cochard B, Flori A, Durand-Gasselin T, Nouy B, Omore A, Pomies V, Riou V, Suryana E, Bouvet JM (2015) Genomic selection prediction accuracy in a perennial crop: case study of oil palm (*Elaeis guineensis* Jacq.). Theor Appl Genet 128(3):397–410

Crossa J, Burgueno J, Dreisigacker S, Vargas M, Herrera-Foessel SA, Lillemo M, Singh RP, Trethowan R, Warburton M, Franco J, Reynolds M, Crouch JH, Ortiz R (2007) Association analysis of historical bread wheat germplasm using additive genetic covariance of relatives and population structure. Genetics 177(3):1889–1913

Crossa J, Campos Gde L, Perez P, Gianola D, Burgueno J, Araus JL, Makumbi D, Singh RP, Dreisigacker S, Yan J, Arief V, Banziger M, Braun HJ (2010) Prediction of genetic values of quantitative traits in plant breeding using pedigree and molecular markers. Genetics 186(2):713–724

Csardi G, Nepusz T (2006) The igraph software package for complex network research. InterJournal 1695(5):1–9

da Silva TA, Cantagalli LB, Saavedra J, Lopes AD, Mangolin CA, Machado MDPD, Scapim CA (2015) Population structure and genetic diversity of Brazilian popcorn germplasm inferred by microsatellite markers. Electron J Biotechnol 18(3):181–187

Da Y, Wang CK, Wang SW, Hu G (2014) Mixed model methods for genomic prediction and variance component estimation of additive and dominance effects using SNP markers. PLoS One 9(1):e87666

Daetwyler HD, Kemper KE, van der Werf JHJ, Hayes BJ (2012) Components of the accuracy of genomic prediction in a multi-breed sheep population. J Anim Sci 90(10):3375–3384

de los Campos G, Sorensen D (2014) On the genomic analysis of data from structured populations. J Anim Breed Genet 131(3):163–164

Edriss V, Gao YX, Zhang XC, Jumbo MB, Makumbi D, Olsen MS, Crossa J, Packard KC, Jannink JL (2017) Genomic prediction in a large African maize population. Crop Sci 57(5):2361–2371

Endelman JB (2015) Ridge regression and other kernels for genomic selection. rrBLUP-package Version: 44

Ertiro BT, Semagn K, Das B, Olsen M, Labuschagne M, Worku M, Wegary D, Azmach G, Ogugo V, Keno T, Abebe B, Chibsa T, Menkir A (2017) Genetic variation and population structure of maize inbred lines adapted to the mid-altitude sub-humid maize agro-ecology of Ethiopia using single nucleotide polymorphic (SNP) markers. BMC Genomics 18(1): 777

Evanno G, Regnaut S, Goudet J (2005) Detecting the number of clusters of individuals using the software STRUCTURE: a simulation study. Mol Ecol 14(8):2611–2620

Fan XM, Bi YQ, Zhang YD, Jeffers DP, Yao WH, Chen HM, Zhao LQ, Kang MS (2015) Use of the suwan1 heterotic group in maize breeding programs in southwestern China. Agron J 107(6):2353–2362

Fernandes EH, Schuster I, Scapim CA, Vieira ESN, Coan MMD (2015) Genetic diversity in elite inbred lines of maize and its association with heterosis. Genet Mol Res 14(2):6509–6517

Frichot E, Francois O (2015) LEA: an R package for landscape and ecological association studies. Methods Ecol Evol 6(8): 925–929

Galinsky KJ, Bhatia G, Loh PR, Georgiev S, Mukherjee S, Patterson NJ, Price AL (2016) Fast principal-component analysis reveals convergent evolution of ADH1B in Europe and East Asia. Am J Hum Genet 98(3):456–472

Gorjanc G, Bijma P, Hickey JM (2015) Reliability of pedigree-based and genomic evaluations in selected populations. Genet Sel Evol 47:65

Granato ISC, Galli G, Couto EGD, Souza MBE, Mendonca LF, Fritsche R (2018) snpReady: a tool to assist breeders in genomic analysis. Mol Breed 38(8):102

Guo Z, Tucker DM, Basten CJ, Gandhi H, Ersoz E, Guo B, Xu Z, Wang D, Gay G (2014) The impact of population structure on genomic prediction in stratified populations. Theor Appl Genet 127(3):749–762

Habier D, Fernando RL, Dekkers JCM (2007) The impact of genetic relationship information on genome-assisted breeding values. Genetics 177(4):2389–2397

Hallauer AR, Carena MJ (2014) Adaptation of tropical maize germplasm to temperate environments. Euphytica 196(1):1–11

Hayes BJ, Bowman PJ, Chamberlain AC, Verbyla K, Goddard ME (2009) Accuracy of genomic breeding values in multi-breed dairy cattle populations. Genet Sel Evol 41:51

He S, Schulthess AW, Mirdita V, Zhao Y, Korzun V, Bothe R, Ebmeyer E, Reif JC, Jiang Y (2016) Genomic selection in a commercial winter wheat population. Theor Appl Genet 129(3):641–651

Huang M, Cabrera A, Hoffstetter A, Griffey C, Van Sanford D, Costa J, McKendry A, Chao S, Sneller C (2016) Genomic selection for wheat traits and trait stability. Theor Appl Genet 129(9):1697–1710

Iheshiulor OOM, Woolliams JA, Yu XJ, Wellmann R, Meuwissen THE (2016) Within- and across-breed genomic prediction using whole-genome sequence and single nucleotide polymorphism panels. Genet Sel Evol 48:15

Isidro J, Jannink JL, Akdemir D, Poland J, Heslot N, Sorrells ME (2015) Training set optimization under population structure in genomic selection. Theor Appl Genet 128(1):145–158

Jan HU, Abbadi A, Lucke S, Nichols RA, Snowdon RJ (2016) Genomic prediction of testcross performance in canola (*Brassica napus*). PLoS One 11(1):e0147769

Janss L, de Los Campos G, Sheehan N, Sorensen D (2012) Inferences from genomic models in stratified populations. Genetics 192(2):693–704

Jombart T, Devillard S, Balloux F (2010) Discriminant analysis of principal components: a new method for the analysis of genetically structured populations. BMC Genet 11:94

Jombart T, Collins C, Kamvar ZN, Lustrik R, Solymos P, Ahmed I, Jombart MT (2015) adegenet: exploratory analysis of genetic and genomic data. R Package Version 201

Karoui S, Carabano MJ, Diaz C, Legarra A (2012) Joint genomic evaluation of French dairy cattle breeds using multiple-trait models. Genet Sel Evol 44:39

Laborda PR, Oliveira KM, Garcia AAF, Paterniani MEA, de Souza AP (2005) Tropical maize germplasm: what can we say about its genetic diversity in the light of molecular markers? Theor Appl Genet 111(7):1288–1299

Lanes ECM, Viana JMS, Paes GP, Paula MFB, Maia C, Caixeta ET, Miranda GV (2014) Population structure and genetic diversity of maize inbreds derived from tropical hybrids. Genet Mol Res 13(3):7365–7376

Lawson DJ, Hellenthal G, Myers S, Falush D (2012) Inference of population structure using dense haplotype data. PLoS Genet 8(1):e1002453

Lehermeier C, Kramer N, Bauer E, Bauland C, Camisan C, Campo L, Flament P, Melchinger AE, Menz M, Meyer N, Moreau L, Moreno-Gonzalez J, Ouzunova M, Pausch H, Ranc N, Schipprack W, Schonleben M, Walter H, Charcosset A, Schon CC (2014) Usefulness of multiparental populations of maize (*Zea mays* L.) for genome-based prediction. Genetics 198(1):3–16

Lehermeier C, Schon CC, de los Campos G (2015) Assessment of genetic heterogeneity in structured plant populations using multivariate whole-genome regression models. Genetics 201(1):323–337

Maenhout S, De Baets B, Haesaert G (2010) Prediction of maize single-cross hybrid performance: support vector machine regression versus best linear prediction. Theor Appl Genet 120(2):415–427

Massman JM, Gordillo A, Lorenzana RE, Bernardo R (2013) Genomewide predictions from maize single-cross data. Theor Appl Genet 126(1):13–22

Mendes MP, de Souza CL (2016) Genomewide prediction of tropical maize single-crosses. Euphytica 209(3):651–663

Molin D, Coelho CJ, Maximo DS, Ferreira FS, Gardingo JR, Matiello RR (2013) Genetic diversity in the germplasm of tropical maize landraces determined using molecular markers. Genet Mol Res 12(1):99–114

Mundim GB, Viana JMS, Maia C, Paes GP, DeLima RO, Valente MSF (2015) Inferring tropical popcorn gene pools based on molecular and phenotypic data. Euphytica 202(1):55–68

Navarro JAR, Wilcox M, Burgueno J, Romay C, Swarts K, Trachsel S, Preciado E, Terron A, Delgado HV, Vidal V, Ortega A, Banda AE, Montiel NOG, Ortiz-Monasterio I, Vicente FS, Espinoza AG, Atlin G, Wenzl P, Hearne S, Buckler ES (2017) A study of allelic diversity underlying flowering-time adaptation in maize landraces. Nat Genet 49(6):970

Nelson PT, Krakowsky MD, Coles ND, Holland JB, Bubeck DM, Smith JSC, Goodman MM (2016) Genetic characterization of the North Carolina State University maize lines. Crop Sci 56(1):259–275

Newell MA, Jannink JL (2014) Genomic selection in plant breeding. In: Fleury D, Whitford R (eds) Crop breeding: methods and protocols. Humana Press/Springer, New Delhi, p 117–130

Olson KM, VanRaden PM, Tooker ME (2012) Multibreed genomic evaluations using purebred Holsteins, jerseys, and Brown Swiss. J Dairy Sci 95(9):5378–5383

Orozco-Ramirez Q, Ross-Ibarra J, Santacruz-Varela A, Brush S (2016) Maize diversity associated with social origin and environmental variation in southern Mexico. Heredity 116(5):477–484

Oyekunle M, Badu-Apraku B, Hearne S, Franco J (2015) Genetic diversity of tropical early-maturing maize inbreds and their

performance in hybrid combinations under drought and optimum growing conditions. Field Crop Res 170:55–65

Patterson N, Price AL, Reich D (2006) Population structure and eigenanalysis. PLoS Genet 2(12):e190

Perez P, de los Campos G (2014) Genome-wide regression and prediction with the BGLR statistical package. Genetics 198(2):483–U463

Porto-Neto LR, Barendse W, Henshall JM, McWilliam SM, Lehnert SA, Reverter A (2015) Genomic correlation: harnessing the benefit of combining two unrelated populations for genomic selection. Genet Sel Evol 47:84

Price AL, Patterson NJ, Plenge RM, Weinblatt ME, Shadick NA, Reich D (2006) Principal components analysis corrects for stratification in genome-wide association studies. Nat Genet 38(8):904–909

Price AL, Zaitlen NA, Reich D, Patterson N (2010) New approaches to population stratification in genome-wide association studies. Nat Rev Genet 11(7):459–463

Purcell S, Neale B, Todd-Brown K, Thomas L, Ferreira MAR, Bender D, Maller J, Sklar P, de Bakker PIW, Daly MJ, Sham PC (2007) PLINK: a tool set for whole-genome association and population-based linkage analyses. Am J Hum Genet 81(3):559–575

Reif JC, Melchinger AE, Xia XC, Warburton ML, Hoisington DA, Vasal SK, Beck D, Bohn M, Frisch M (2003) Use of SSRs for establishing heterotic groups in subtropical maize. Theor Appl Genet 107(5):947–957

Riedelsheimer C, Czedik-Eysenberg A, Grieder C, Lisec J, Technow F, Sulpice R, Altmann T, Stitt M, Willmitzer L, Melchinger AE (2012) Genomic and metabolic prediction of complex heterotic traits in hybrid maize. Nat Genet 44(2): 217–220

Riedelsheimer C, Endelman JB, Stange M, Sorrells ME, Jannink JL, Melchinger AE (2013) Genomic predictability of interconnected biparental maize populations. Genetics 194(2): 493–503

Rincent R, Laloe D, Nicolas S, Altmann T, Brunel D, Revilla P, Rodriguez VM, Moreno-Gonzalez J, Melchinger A, Bauer E, Schoen CC, Meyer N, Giauffret C, Bauland C, Jamin P, Laborde J, Monod H, Flament P, Charcosset A, Moreau L (2012) Maximizing the reliability of genomic selection by optimizing the calibration set of reference individuals: comparison of methods in two diverse groups of maize inbreds (*Zea mays* L.). Genetics 192(2):715–728

Rincent R, Nicolas S, Bouchet S, Altmann T, Brunel D, Revilla P, Malvar RA, Moreno-Gonzalez J, Campo L, Melchinger AE, Schipprack W, Bauer E, Schoen CC, Meyer N, Ouzunova M, Dubreuil P, Giauffret C, Madur D, Combes V, Dumas F, Bauland C, Jamin P, Laborde J, Flament P, Moreau L, Charcosset A (2014) Dent and Flint maize diversity panels reveal important genetic potential for increasing biomass production. Theor Appl Genet 127(11):2313–2331

Rincent R, Charcosset A, Moreau L (2017) Predicting genomic selection efficiency to optimize calibration set and to assess prediction accuracy in highly structured populations. Theor Appl Genet 130(11):2231–2247

Roberts DW (2016) labdsv: ordination and multivariate analysis for ecology. R Package Version 16–1

Roorkiwal M, Rathore A, Das RR, Singh MK, Jain A, Srinivasan S, Gaur PM, Chellapilla B, Tripathi S, Li Y, Hickey JM, Lorenz A, Sutton T, Crossa J, Jannink JL, Varshney RK (2016) Genome-enabled prediction models for yield related traits in chickpea. Front Plant Sci 7:1666

Saatchi M, McClure MC, McKay SD, Rolf MM, Kim J, Decker JE, Taxis TM, Chapple RH, Ramey HR, Northcutt SL, Bauck S, Woodward B, Dekkers JCM, Fernando RL, Schnabel RD, Garrick DJ, Taylor JF (2011) Accuracies of genomic breeding values in American Angus beef cattle using K-means clustering for cross-validation. Genet Sel Evol 43:1–16

Santos JPR, Vasconcellos RCD, Pires LPM, Balestre M, Von Pinho RG (2016) Inclusion of dominance effects in the multivariate GBLUP model. PLoS One 11(4):1–21

Schaefer CM, Bernardo R (2013) Population structure and single nucleotide polymorphism diversity of historical Minnesota maize inbreds. Crop Sci 53(4):1529

Schulz-Streeck T, Ogutu JO, Karaman Z, Knaak C, Piepho HP (2012) Genomic selection using multiple populations. Crop Sci 52(6):2453–2461

Sousa MBE, Cuevas J, Couto EGD, Perez-Rodriguez P, Jarquin D, Fritsche-Neto R, Burgueno J, Crossa J (2017) Genomic-enabled prediction in maize using kernel models with genotype x environment interaction. G3-Genes Genom Genet 7(6):1995–2014

Spindel J, Begum H, Akdemir D, Virk P, Collard B, Redona E, Atlin G, Jannink JL, McCouch SR (2015) Genomic selection and association mapping in Rice (*Oryza sativa*): effect of trait genetic architecture, training population composition, marker number and statistical model on accuracy of rice genomic selection in elite, tropical rice breeding lines. PLoS Genet 11(2):e1004982

Sukumaran S, Xiang W, Bean SR, Pedersen JF, Kresovich S, Tuinstra MR, Tesso TT, Hamblin MT, Yu J (2012) Association mapping for grain quality in a diverse sorghum collection. Plant Genome 5(3):126–135

Sukumaran S, Dreisigacker S, Lopes M, Chavez P, Reynolds MP (2015) Genome-wide association study for grain yield and related traits in an elite spring wheat population grown in temperate irrigated environments. Theor Appl Genet 128(2): 353–363

Technow F, Riedelsheimer C, Schrag TA, Melchinger AE (2012) Genomic prediction of hybrid performance in maize with models incorporating dominance and population specific marker effects. Theor Appl Genet 125(6):1181–1194

Teixeira JEC, Weldekidan T, de Leon N, Flint-Garcia S, Holland JB, Lauter N, Murray SC, Xu W, Hessel DA, Kleintop AE, Hawk JA, Hallauer A, Wisser RJ (2015) Hallauer's Tuson: a decade of selection for tropical-to-temperate phenological adaptation in maize. Heredity 114(2):229–240

Thomasen JR, Sorensen AC, Su G, Madsen P, Lund MS, Guldbrandtsen B (2013) The admixed population structure in Danish Jersey dairy cattle challenges accurate genomic predictions. J Anim Sci 91(7):3105–3112

Tucker G, Price AL, Berger B (2014) Improving the power of GWAS and avoiding confounding from population stratification with PC-Select. Genetics 197(3):1045–1049

Unterseer S, Bauer E, Haberer G, Seidel M, Knaak C, Ouzunova M, Meitinger T, Strom TM, Fries R, Pausch H, Bertani C, Davassi A, Mayer KFX, Schon CC (2014) A powerful tool for genome analysis in maize: development and evaluation of the high density 600 k SNP genotyping array. BMC Genomics 15(823):1–15

Unterseer S, Pophaly SD, Peis R, Westermeier P, Mayer M, Seidel MA, Haberer G, Mayer KFX, Ordas B, Pausch H, Tellier A, Bauer E, Schon CC (2016) A comprehensive study of the genomic differentiation between temperate Dent and Flint maize. Genome Biol 17:137

VanRaden PM (2008) Efficient methods to compute genomic predictions. J Dairy Sci 91(11):4414–4423

Ventura R, Larmer S, Schenkel FS, Miller SP, Sullivan P (2016) Genomic clustering helps to improve prediction in a multibreed population. J Anim Sci 94(5):1844–1856

Wang ML, Sukumaran S, Barkley NA, Chen ZB, Chen CY, Guo BZ, Pittman RN, Stalker HT, Holbrook CC, Pederson GA, Yu JM (2011) Population structure and marker-trait association analysis of the US peanut (*Arachis hypogaea* L.) mini-core collection. Theor Appl Genet 123(8):1307–1317

Wientjes YCJ, Bijma P, Vandenplas J, Calus MPL (2017) Multi-population genomic relationships for estimating current genetic variances within and genetic correlations between populations. Genetics 207(2):503–515

Windhausen VS, Atlin GN, Hickey JM, Crossa J, Jannink JL, Sorrells ME, Raman B, Cairns JE, Tarekegne A, Semagn K, Beyene Y, Grudloyma P, Technow F, Riedelsheimer C, Melchinger AE (2012) Effectiveness of genomic prediction of maize hybrid performance in different breeding populations and environments. G3-Genes Genom Genet 2(11): 1427–1436

Wu YS, Vicente FS, Huang KJ, Dhliwayo T, Costich DE, Semagn K, Sudha N, Olsen M, Prasanna BM, Zhang XC, Babu R (2016) Molecular characterization of CIMMYT maize inbred lines with genotyping-by-sequencing SNPs. Theor Appl Genet 129(4):753–765

Yan JB, Shah T, Warburton ML, Buckler ES, McMullen MD, Crouch J (2009) Genetic characterization and linkage disequilibrium estimation of a global maize collection using SNP markers. PLoS One 4(12):e8451

Yang XH, Gao SB, Xu ST, Zhang ZX, Prasanna BM, Li L, Li JS, Yan JB (2011) Characterization of a global germplasm collection and its potential utilization for analysis of complex quantitative traits in maize. Mol Breed 28(4):511–526

Yu JM, Pressoir G, Briggs WH, Bi IV, Yamasaki M, Doebley JF, McMullen MD, Gaut BS, Nielsen DM, Holland JB, Kresovich S, Buckler ES (2006) A unified mixed-model method for association mapping that accounts for multiple levels of relatedness. Nat Genet 38(2):203–208

Yu X, Li X, Guo T, Zhu C, Wu Y, Mitchell SE, Roozeboom KL, Wang D, Wang ML, Pederson GA, Tesso TT, Schnable PS, Bernardo R, Yu J (2016) Genomic prediction contributing to a promising global strategy to turbocharge gene banks. Nat Plants 2:16150

Zhang J, Song Q, Cregan PB, Jiang GL (2016) Genome-wide association study, genomic prediction and marker-assisted selection for seed weight in soybean (Glycine max). Theor Appl Genet 129(1):117–130

Zheng X, Levine D, Shen J, Gogarten SM, Laurie C, Weir BS (2012) A high-performance computing toolset for relatedness and principal component analysis of SNP data. Bioinformatics 28(24):3326–3328

Zhou L, Lund MS, Wang Y, Su G (2014) Genomic predictions across Nordic Holstein and Nordic Red using the genomic best linear unbiased prediction model with different genomic relationship matrices. J Anim Breed Genet 131(4):249–257

Zhu C, Yu J (2009) Nonmetric multidimensional scaling corrects for population structure in association mapping with different sample types. Genetics 182(3):875–888